ELSEVIER

Combustion and Flame 132 (2003) 723–741

Combustion and Flame

NO_x emissions in n-heptane/air partially premixed flames

Hongshe Xue, Suresh K. Aggarwal*

Department of Mechanical and Industrial Engineering (M/C 251), University of Illinois at Chicago, 842 W. Taylor St., Chicago IL 60607-7022, USA

Received 11 January 2002; received in revised form 21 October 2002; accepted 6 November 2002

Abstract

NO_x emissions in n-heptane/air partially premixed flames (PPFs) in a counter-flow configuration have been investigated. The flame is computed using a detailed mechanism that combines the Held's mechanism for n-heptane and the Li and Williams' mechanism for NO_x. The combined mechanism contains 54 species and 327 reactions. Based on a detailed analysis, dominant mechanisms responsible for NOx formation and destruction in PPFs are found to be thermal, prompt, and reburn mechanisms. The dominant reactions associated with these mechanisms are also identified. The effects of strain rate (a_s) and equivalence ratio (ϕ) on NO_x emissions are characterized for conditions in which the flame contains two spatially separated reaction zones; a rich premixed zone on the fuel side and a non-premixed zone on the air side. For most conditions, except for relatively high level of partial premixing, the NO formation rate in the non-premixed zone is significantly higher than that in the rich premixed zone. Within the rich premixed zone, the contribution of thermal NO to total NO_x is higher than that of prompt NO, while in the non-premixed zone, the prompt NO is the major contributor. The behavior is related to the transport of acetylene from the rich premixed to the non-premixed zone, and higher concentrations of CH, O, and OH radicals in the latter zone. A notable result in this context is that the existence of CH does not automatically imply that prompt NO will form. The existence of O and OH is also necessary, in addition to CH, to form prompt NO. The relative contributions of thermal and prompt mechanisms to total NO_x are generally insensitive to variations in a_s, but show strong sensitivity to variations in ϕ. There is a NO_x destruction region sandwiched between the rich premixed and the non-premixed reaction zones. The NO_x destruction occurs mainly through the reburn mechanism. The NO_x emission index (EINOx) is computed as a function of ϕ and a_s. These results are qualitatively in accord with previous numerical and experimental results for methane-air PPFs.

Keywords: NO_x emissions; Heptane partially premixed flames; Detailed chemistry

1. Introduction

Partially premixed flames (PPFs) are established when less than stoichiometric quantity of oxidizer is molecularly mixed with the fuel stream before entering the reaction zone where additional oxidizer is available for complete combustion. PPFs occur widely in practical combustion systems either by design or under conditions arising due to various phenomena, such as poor mixing, spray vaporization [1], flame lift-off [2], and local extinction followed by reignition in turbulent flames [3].

Due to their immense practical and fundamental importance, PPFs have been studied extensively in recent years [4–15]. Most of the studies have focused, however, on the structure rather than the emission characteristics of these flames. This is rather

Corresponding author. Tel.: +1-312-996-2235; fax: +1-312-413-0447.

E-mail address: ska@uic.edu (S.K. Aggarwal).

0010-2180/03/$ – see front matter
doi: 10.1016/S0010-2180(02)00534-5

surprising considering that PPFs occur in many combustion systems, and may have superior emission characteristics compared to premixed and non-premixed flames. The favorable emission characteristics are related to the presence of multiple reaction zones that characterize PPFs. Because interactions between the reaction zones can be modified by varying stoichiometry and transport, it offers the possibility of optimizing soot and NOx emissions in these flames.

In the present study, we investigate NOx emissions in heptane-air PPFs. Previous investigations dealing with NOx emissions in PPFs have mostly considered methane-air flames. Gore and Zhan [7] measured emission indices for NO_x, CO and HC in laminar, axisymmetric methane-air flames. An important result from this study was the existence of an optimum level of partial premixing that yielded the lowest NOx emission index, for a fixed fuel flow rate and overall equivalence ratio.[1] A similar result was reported by Kim et al. [8] in their investigation of laminar ethane-air PPFs. They surmised that the existence of a minimum NOx emission index at $\phi = 2.2$ was due to a competition between prompt and thermal mechanisms. At higher level of partial premixing ($\phi < 2.2$), the rich premixed zone accounted for most of NO that was formed primarily due to the prompt mechanism, while at lower level of mixing ($\phi > 2.2$), most of NO was formed in the non-premixed reaction zone, where thermal mechanism was the dominant contributor.

Blevins and Gore [9] reported a numerical investigation of NO formation in a low strain rate counterflow methane-air PPF. The NO emission was found to depend strongly on the flame structure, which was determined by the level of partial premixing. For a range of equivalence ratios that yielded a double flame structure, they identified two NO formation zones and one NO destruction zone. In addition, the computed NO_x emission index indicated a maximum value near $\phi \approx 2.2$. This peak was not observed, however, in the numerical study of Nishioka et al. [10]. The difference is perhaps attributable to different strain rates used in the two investigations.

Li and Williams [11] conducted a detailed experimental and numerical investigation of methane-air PPFs, and characterized the effects of partial premixing and additives (H_2O, CO_2, N_2, and Ar) on NO_x emissions. For the conditions investigated, the prompt mechanism was observed to play a more dominant role in NO_x formation. The result was, however, in variance with that reported by Kim et al. [8] who observed that the dominant NOx mechanism changes from prompt to thermal as the level of partial premixing is reduced.

Nguyen et al. [12] reported measurements of NO concentration in co-flowing partially premixed methane-air flames using Raman and Rayleigh scattering, and laser-induced fluorescence (LIF). Radial and axial profiles of NO concentration were obtained for three equivalence ratios. It was observed that the peak NO value decreased as the equivalence ratio was increased.

Our literature review indicates that fundamental aspects concerning the effects of stoichiometry and transport on NOx emissions in PPFs are presently not well understood. For instance, the relative contributions of thermal, prompt, and other mechanisms to total NOx at different levels of partial premixing and flow straining have not been characterized. While the existence of an optimum equivalence ratio has been reported by some researchers [7, 8], it has not been confirmed by others [9–11]. Previous studies have mainly focused on methane-air PPFs. Investigations of higher hydrocarbon PPFs, in which the NOx emission is a more serious concern, have not been reported.

The major objective of this study is to examine the NOx behavior of heptane-air PPFs. In particular, the investigation focuses on (1) characterizing the dominant NOx production/destruction mechanisms and associated pathways in various regions of a PPF, and (2) examining the existence of an optimum level of partial premixing for minimum NOx in PPFs. The n-heptane fuel is considered, because it is deemed as the most representative of the liquid hydrocarbon fuels, and a good surrogate for practical fuels. Moreover, its oxidation chemistry has been extensively investigated [15–19]. A counter-flow configuration is employed, because it facilitates a detailed investigation of the relative importance of various reaction zones in the NOx formation and destruction processes. For example, because the spatial region between the two reaction zones is generally devoid of O_2 and O species, it may represent a destruction zone for NO. The role of this region in the overall production or destruction of NO has not been examined in previous studies. Moreover, the effects of stoichiometry and transport (strain rate) can be more easily separated in this geometry.

Previous investigations of heptane-air PPFs [14, 15, 20] have mostly focused on the detailed structure of partially premixed flames containing two reaction zones. To the best of our knowledge, except for one recent study [15], the NOx characteristics of these flames have not been investigated previously.

2. Physical-numerical model

A partially premixed flame in a counter-flow configuration is considered. The flame is established by igniting a fuel-air mixture that is formed by two

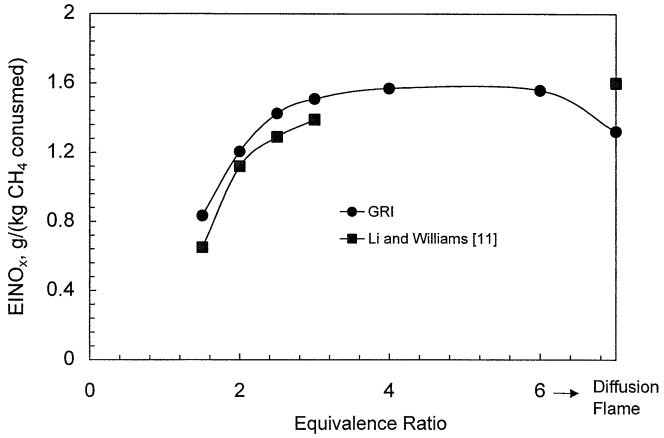

Fig. 1. NOx emission index versus ϕ for methane-air partial premixed flames, computed by combining the Li and Williams' NOx mechanism with the GRI-Mech 2.11. The predictions of Li and Williams are also shown.

opposing jets, one containing a rich n-heptane/air mixture and the other containing air. In this configuration, a schematic of which can be found in Refs [14, 20], the flame is observed to contain two spatially separated reaction zones; a rich premixed reaction zone on the fuel side and a non-premixed reaction zone on the air side.

Simulations are performed using the Oppdif [21] and Chemkin packages [22]. Oppdif is a Fortran program that computes the flow field in a counterflow configuration. The detailed description of Oppdif can be found in the Sandia manual. An optically thin radiation model was incorporated into the original Oppdif code to account for the radiation heat loss. Details of this model can be found elsewhere [6].

3. The chemical kinetics model

Both semi-detailed and detailed mechanisms have been proposed for n-heptane chemistry [15–19]. The present study employs the semi-detailed mechanism developed by Held et al. [17]. The mechanism has been extensively validated against flow reactor, shock tube, stirred reactor, and laminar flame speed experimental data [17, 18]. We have reported additional validations [20] using the experimental data for laminar flame speeds, and the structure of a prevaporized heptane non-premixed flame. Li and Williams [14] have also used a semi-detailed mechanism that is essentially based on the Held's mechanism and reported good agreement between the measured and predicted heptane-air partially premixed flame structures.

Several detailed mechanisms are also available for the NO_x chemistry. These include the NO_x mechanism used in GRI-Mech 3.0 [23], Li and Williams' mechanism [11], Warnatz mechanism [24], Leeds mechanism [25], and mechanisms discussed by Miller and Bowman [26]. Bajaj [27] performed a comprehensive comparison of the first three mechanisms for methane-air PPFs, and found the Li and Williams' mechanism to reproduce experimental data better than the other two mechanisms. In addition, Li and Williams reported excellent agreement between the measured and predicted NOx profiles using their mechanism for methane-air PPFs.

The feasibility of combining the Li and Williams' NOx mechanism with other hydrocarbon fuel oxidation mechanisms was further tested by combining this mechanism with the GRI-Mech 2.11, and using the combined mechanism to predict the NOx emission index for methane-air PPFs. The emission index is defined as [28]

$$EINO_x = \frac{\int_0^L MW_{NO_x}\dot{\omega}_{NO_x}dx}{-\int_0^L MW_{C_7H_{16}}\dot{\omega}_{C_7H_{16}}dx} \quad (1)$$

Here MW represents the molecular weight, $\dot{\omega}$ the reaction rate, L the separation distance between the two nozzles, and x the axial coordinate. Figure 1 presents EINOx calculated using the combined mechanism and plotted versus the equivalence ratio (ϕ). The EINOx values reported by Li and Williams are also shown. Except for some differences at high ϕ values, there is generally good agreement between the two results. Based on these considerations, the present study combines the Li and Williams' NO_x mechanism with the Held's n-heptane mechanism.

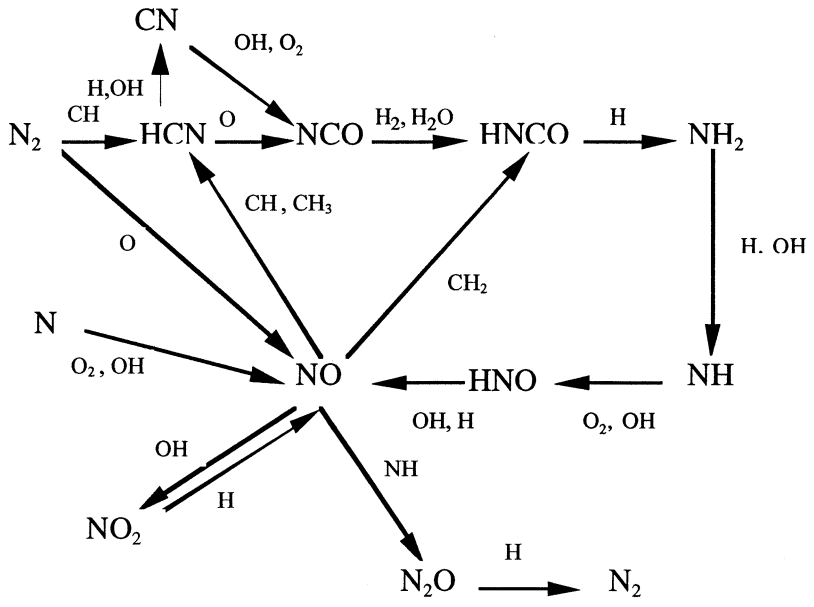

Diagram

The combined mechanism consists of 327 elementary reactions that involve 54 species.

4. Results

4.1. The general NO_x formation path

The heptane-air partially premixed flames were simulated for various conditions, and the ROPA (Rate of Production Analysis) methodology [29] was employed to identify dominant reactions that make major contribution to the production rate of a given species. Based on this analysis, the general NOx mechanism in the two reaction zones are summarized in the diagram above.

Generally, five mechanisms are involved in the NOx production in hydrocarbon flames, namely, the thermal, the prompt, the NO_2, the N_2O, and the reburn mechanisms. The major contribution to NO come from the reaction of N with O_2 or OH, and the reaction of N_2 with O, that is, the thermal mechanism, and from the reactions associated with the chain from N_2 to HCN and down to NO, that is, the prompt mechanism. Thus the diagram includes both the prompt NO and thermal NO pathways. In addition, the diagram indicates paths that consume NO producing HCN and HNCO, which are also referred to as the reburn mechanism of NO. The relative contribution of each mechanism to total NOx under different conditions is characterized in the following sections.

4.2. The effect of strain rate on NO formation

Figure 2 presents the computed flame structure for three PPFs established at different strain rates, a_s = 50, 100, and 150 s^{-1}, but at a fixed ϕ = 2.0. The profiles of temperature, and CH and NO mole fraction are shown. Locations of the two reaction zones, namely the rich premixed and the non-premixed zones, can be identified from the temperature profiles. As a_s is increased, the rich premixed zone moves downstream, reducing the separation distance between the two reaction zones. For a_s = 150 s^{-1}, the two reaction zones are in the process of merging. As discussed previously in our numerical study [20], and observed experimentally by Li and Williams [14], n-heptane is partially oxidized in the rich premixed zone to yield H_2, CO, and C_2H_2, which are transported to and represent the "fuels" for the non-premixed zone. Based on the ROPA [29] analysis, it was observed that C_2H_2 is converted into CH_2, and HCCO, with the latter subsequently converted into CH_2. An examination of CH_2 formation reactions indicated that CH_2 is almost entirely produced by C_2H_2 and HCCO. Other reactions involved in the production of CH_2 contribute less than 5%. Because CH mainly comes from CH_2, it can be concluded that C_2H_2 is the major source of CH. Consequently, the transport of C_2H_2 to the non-premixed zone is also indicated by the second peak in CH mole fraction profile in this zone.

The CH profiles exhibit two peaks with comparable heights. The first peak is associated with the

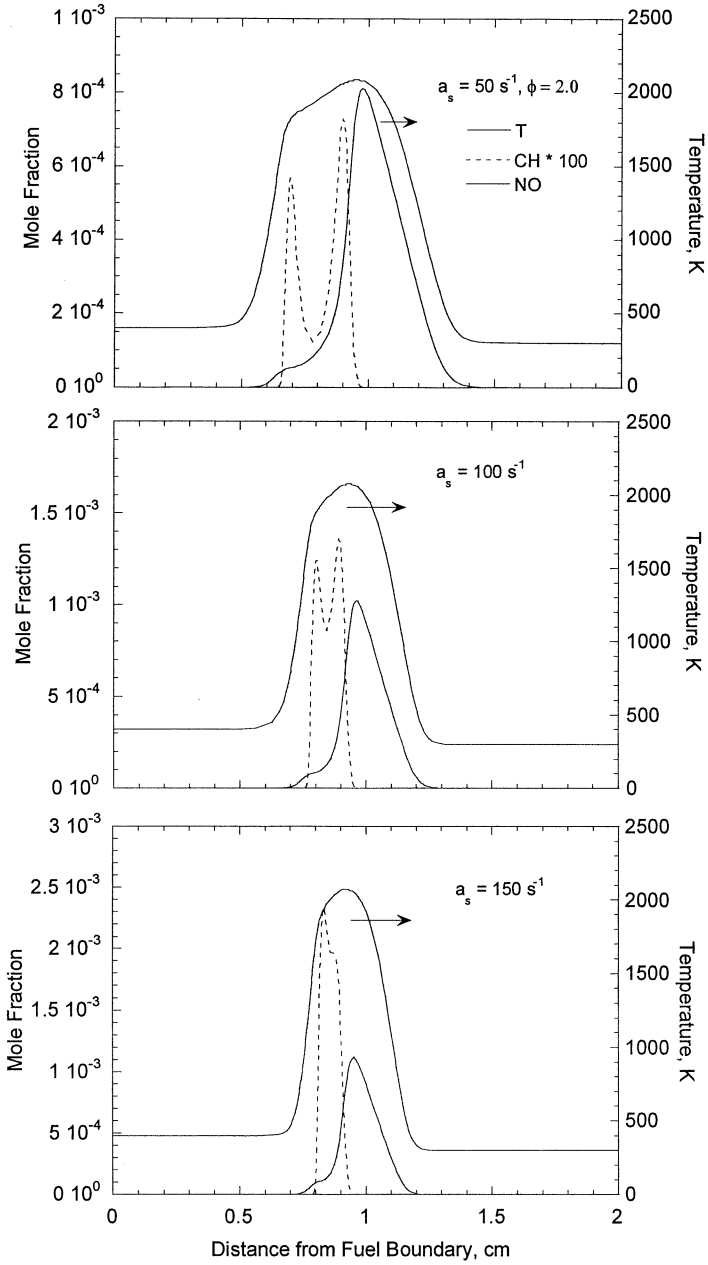

Fig. 2. Profiles of temperature, and CH and NO mole fractions for heptane-air partially premixed flames established at a_s = 50, 100, 150 s^{-1}, and $\phi = 2.0$.

fuel oxidation chemistry that yields CO, H_2, and C_2H_2 in the rich premixed zone, while the second peak is associated with the transport of acetylene from the rich premixed to the non-premixed zone. Because CH is largely responsible for the prompt NO, this species characterizes interactions between the two reaction zones in the context of NO emissions from PPFs.

Important observation from Fig. 2 is that while the CH profile exhibits two peaks, the NO profile contains one dominant peak that is located in the non-premixed zone. This implies that the presence of CH does not lead to a significant production of NO in the rich premixed zone, which can be attributed to the paucity of O and OH radicals in this zone, as discussed later in this section. Thus, most of NO is produced in the non-premixed zone. This is confirmed by the NO production rate profiles presented

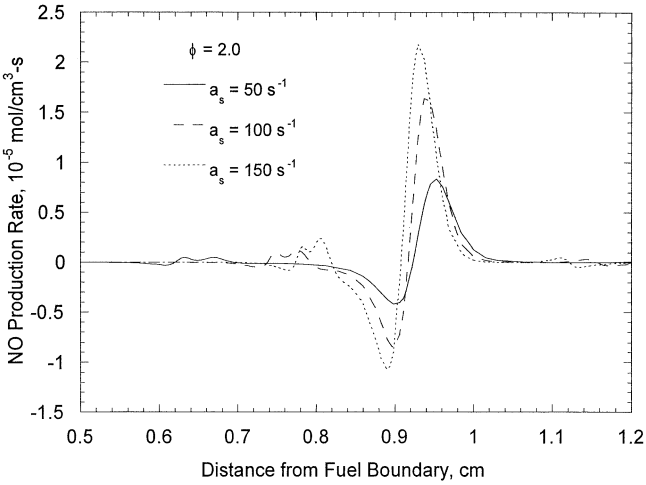

Fig. 3. Profiles of NO production rate for three PPFs discussed in the context of Fig. 2.

in Fig. 3. These profiles also indicate that NO production rate in both the rich premixed and non-premixed zones increases as the strain rate is increased. The production rate in the non-premixed zone is, however, significantly higher than that in the rich premixed zone. In addition, there is a NO consumption zone that is sandwiched between the rich premixed and the non-premixed zones. The NO consumption occurs mainly through the reburn mechanism.

The ROPA method [28] was performed using KINALC [29] to examine the relative contribution of each mechanism to total NOx. Based on this analysis [29, 30], the important contributors to total NOx were found to be the thermal, prompt, and reburn mechanisms. The contributions of NO_2 mechanism and N_2O mechanism were found to be negligible. The ROPA method was also employed to identify dominant reactions (pathways) associated with the thermal, prompt, and reburn mechanisms. The analysis yielded the following dominant reactions for the thermal mechanism:

$$O + N_2 \leftrightarrow NO + N \quad \text{(R1)}$$

$$N + O_2 \leftrightarrow NO + O \quad \text{(R2)}$$

$$N + OH \leftrightarrow NO + H \quad \text{(R3)}$$

while the prompt NO mechanism involved the following main reactions:

$$HNO + M \leftrightarrow H + NO + M \quad \text{(R4)}$$

$$HNO + H \leftrightarrow NO + H_2 \quad \text{(R5)}$$

$$HNO + OH \leftrightarrow NO + H_2O \quad \text{(R6)}$$

$$NCO + O \leftrightarrow NO + CO \quad \text{(R7)}$$

$$NH + O \leftrightarrow NO + H \quad \text{(R8)}$$

and the reburn mechanism involved the following reactions:

$$NO + CH_2 \leftrightarrow HNCO + H \quad \text{(R9)}$$

$$NO + CH \leftrightarrow HCN + O \quad \text{(R10)}$$

$$NO + CH_3 \leftrightarrow HCN + H_2O \quad \text{(R11)}$$

Figure 4a presents the profiles of NO production/consumption rates for the thermal, prompt, and reburn mechanisms for a PPF established at $a_s = 100\ s^{-1}$ and $\phi = 2.0$. The profiles of some key species and temperature for this case are presented in Fig. 4b. Plots similar to those presented in Fig. 4 were obtained for other strain rates, but are not shown. Important observations from Figs. 3 and 4 are:

1. For the conditions investigated, the amount of NO formed in the non-premixed zone is significantly higher than that in the rich premixed zone; see Fig. 3. As indicated in Fig. 4b, this is due to the paucity of OH and O radicals in the latter zone. Another consequence of the lack of these radicals is that the reburn mechanism that consumes NO becomes important, and this decreases the net NO formed in the rich premixed zone. This is evident in the profile of reburn NO rate presented in Fig. 4a.
2. In general, the contribution of thermal NO exceeds that of prompt NO in the rich premixed zone, while prompt mechanism is generally the major contributor of NO in the non-premixed zone. Further insight into this behavior is provided by the comparison of CH profiles in Fig. 2 and HCN production rate profiles in Fig. 4. The HCN production rate is calculated using reactions R10 and R11, and the prompt NO initiation step

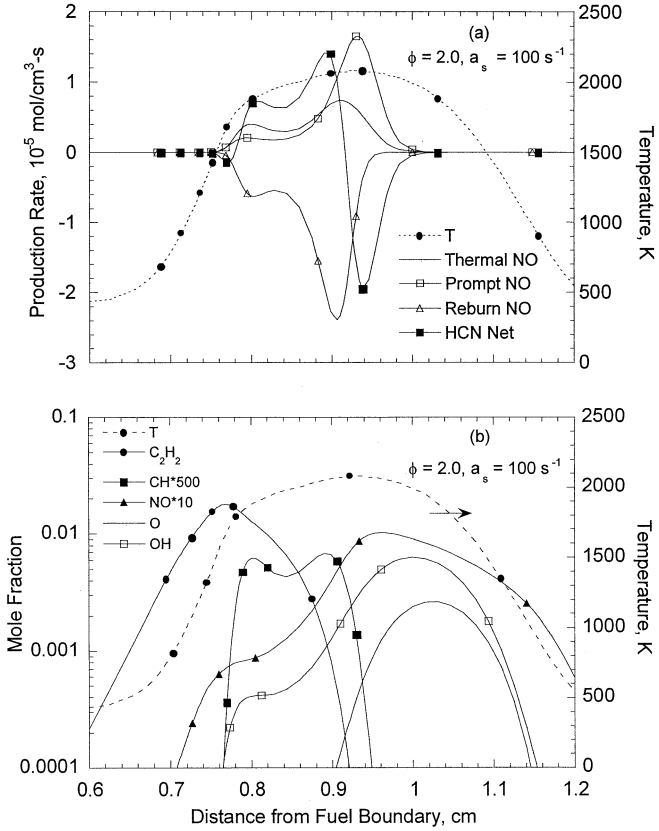

Fig. 4. (a) NO production/destruction rate for the thermal, prompt, and reburn mechanisms plotted versus distance from the fuel nozzle for $\phi = 2.0$, and $a_s = 100\ s^{-1}$. Locations of the two reaction zones are indicated by the temperature profile, and HCN production rate profile is also shown. (b) Profiles of temperature and species mole fractions for conditions of Fig. 4a.

$$CH + N_2 \leftrightarrow HCN + N \qquad (R12)$$

As noted earlier, C_2H_2 provides CH radicals in both the reaction zones. This is also evident in the C_2H_2 and CH profiles presented in Fig. 4b. As soon as CH radicals become available from hydrocarbon reactions, they form HCN through reaction R12, which is indicated by the fact that the respective CH peaks coincide with the HCN production rate peaks. However, the HCN consumption in Fig. 4a indicates that the subsequent conversion of HCN to NO through the NCO path mainly occurs in the non-premixed reaction zone due to the availability of O and OH radicals in that zone. Consequently, while the amount of HCN produced in the rich premixed zone is comparable to that in the non-premixed zone, the prompt NO is only significant in the non-premixed zone due to the availability of O and OH radicals in this zone.

3. The thermal NO profile has two peaks, corresponding to the rich premixed and non-premixed reaction zones. Because O and OH are the key radicals for thermal NO, and also represent an important part of hydrocarbon chemistry that characterizes partially premixed flames, the behavior of thermal NO is, therefore, directly related to the flame structure with respect to its response to strain rate.
4. The locations of the peak thermal and prompt NO rates do not coincide. In the rich premixed zone, the prompt NO peak precedes (i.e., nearer to the fuel boundary) the thermal NO peak. As a consequence, the NO production rate profile in the premixed zone has a 'M' shape (Fig. 3). In the non-premixed zone, the thermal NO peak precedes the prompt NO peak. The location of each peak is determined by the distribution of CH, OH, and O radicals.
5. As noted earlier, the consumption of NO occurs through the reburn mechanism and involves conversion of NO to HCN and HNCO

Table 1
Relative contribution of thermal and prompt mechanisms at different strain rates, and a fixed $\phi = 2.0$

	$a_s = 50\ s^{-1}$	$a_s = 100\ s^{-1}$	$a_s = 150\ s^{-1}$
Contribution of thermal NO (%)	39.8	40	41
Contribution of prompt NO (%)	60.2	60	59

through reactions R9-R11. Among these three reactions, the first two involving the consumption of NO through CH and CH_2 are more dominant. Because both CH and CH_2 are available in the rich premixed zone as well as in the region just upstream of the non-premixed zone, the NO consumption rate profile has two peaks, as indicated in Fig. 4a. The first peak is responsible for reducing the net NO formation rate in the rich premixed zone. The region containing the second peak is located just upstream of the non-premixed reaction zone, and represents the major NO destruction region.

In summary, both the thermal and prompt mechanisms are closely related to the availability of OH, O and CH radicals. This has two important implications. First, the thermal NO becomes the major contributor to total NOx in the rich premixed zone, while the prompt NO becomes the dominant contributor in the non-premixed zone. Second, the effect of strain rate on NO formation can be inferred from its effect on the distribution of these radicals, that is, on the partially premixed flame structure. In a previous study [20], we have shown that the structure of n-heptane partially premixed flames is relatively insensitive to variations in the strain rate, except for very low[3] and critical (merging and extinction) values of strain rates. Consequently, the relative contributions of thermal and prompt mechanisms to total NOx should not show significant variation with the strain rate. This observation is confirmed by the data presented in Table 1, which shows the relative contributions of thermal and prompt NO, obtained by integrating the respective reaction rate profiles.

It is also important to mention that Nishioka et al. [31] examined the role of key elementary reactions in the relative contributions of three dominant NO mechanisms. The focus of our work is, however, different than that of the cited study. While Nishioka et al. focused on the effect of the flame type (premixed, diffusion, or double flame) on NO formation processes, our work aims to characterize the effects of partial premixing (ϕ) and strain rate on NOx formation in partially premixed flames.

4.3 The effect of equivalence ratio on NO formation

Figure 5 presents the profiles of temperature, and CH and NO mole fractions for PPFs established at $\phi = 1.5$, 2.0, and 2.5, and $a_s = 100\ s^{-1}$. The corresponding NO formation rate profiles are shown in Fig. 6. As ϕ is increased, the NO formation rate in the rich premixed zone decreases, while that in the non-premixed zone increases. This is attributed to two factors. First, the radical activity is reduced in the premixed zone but enhanced in the non-premixed zone as the level of partial premixing is decreased, or ϕ is increased. The change in radical activity was confirmed by plotting O and OH mole fraction profiles. Second, the transport of acetylene from the premixed to the non-premixed zone is enhanced, which increases the availability of CH species in the non-premixed zone, and, thus, enhances the prompt NO formation in this zone.

Figure 7 presents the NO reaction rate profiles for the thermal, prompt, and reburn mechanisms for three different equivalence ratios. The locations of the two reaction zones (with the premixed zone on the left) are indicated with vertical bars in Fig. 7a. With the increase in ϕ, the NO formation/destruction rates for all three mechanisms decrease in the rich premixed zone, while they increase in the non-premixed zone. This is consistent with the variation of total NO formation rate with ϕ, and can be attributed to the increased concentration of CH, O and OH radicals in the non-premixed zone. In addition, as ϕ is increased, the contribution from prompt mechanism increases, while that from thermal mechanism decreases. This is again due to the enhanced transport of acetylene to the non-premixed zone with the increase in ϕ, which increases the concentration of CH radicals in the non-premixed zone. Table 2 summarizes the respective contributions of thermal and prompt mechanisms for different ϕ.

4.4. Global effects of strain rate and equivalence ratio

To examine the global effects of a_s and ϕ on NO contributions from the three mechanisms in the rich premixed and non-premixed zones, we present in

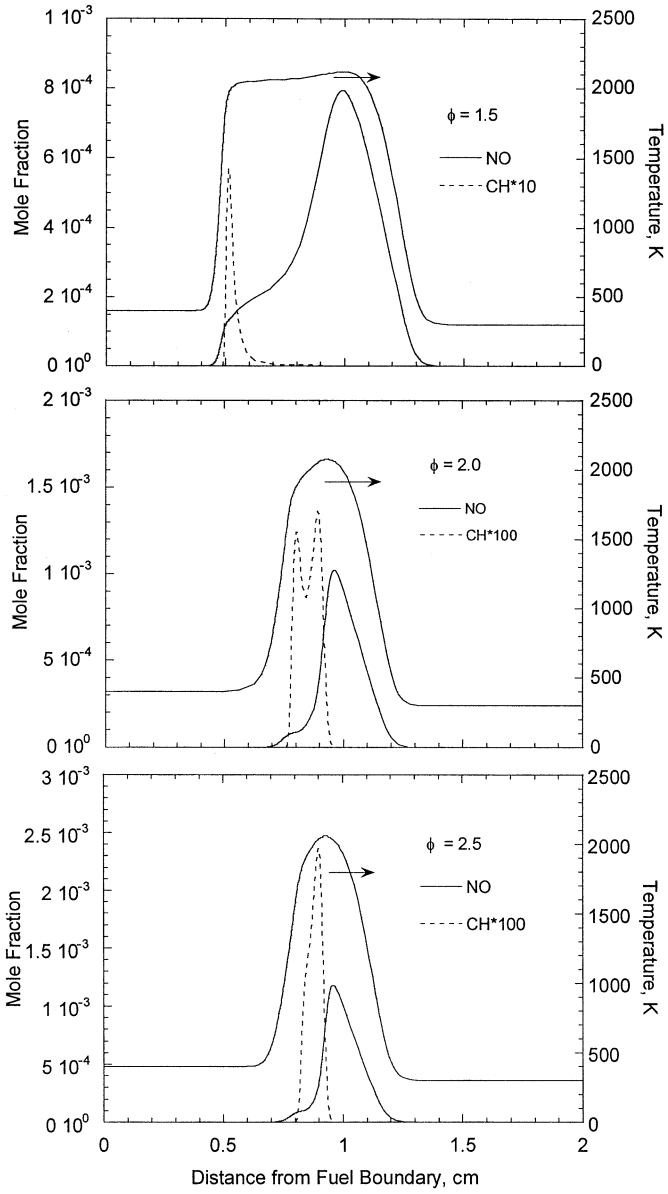

Fig. 5. Profiles of temperature, and CH and NO mole fractions for heptane-air partially premixed flames established at ϕ = 1.5, 2.0, 2.5, and $a_s = 100\ s^{-1}$.

Figs. 8 and 9 the total production rates of NO obtained by integrating the NO production rate along the axial direction (X). Figures 8a and b present the total production rate in the rich premixed and non-premixed zones, respectively, for the thermal, prompt, reburn (absolute value), and the net NO plotted versus the strain rate. As a_s is increased, the NO production rates for all three mechanisms increase. However, the rate of reburn NO increases faster than those of the other two and consequently the net NO production rate in the rich premixed zone decreases as a_s is increased. For low strain rates (a_s = 50 s^{-1}), the rich premixed zone produces NO, whereas for high strain rates ($a_s \geq 100\ s^{-1}$), it consumes NO. In the non-premixed zone, the NO production rate for all three mechanisms as well as the net NO production rate increase as a_s is increased, see Fig. 8b As noted earlier, thermal NO exceeds prompt NO in the rich premixed zone, while prompt NO exceeds thermal NO in the non-premixed zone. Overall, the total NO production in the non-premixed zone far exceeds that in the rich premixed zone. This is due

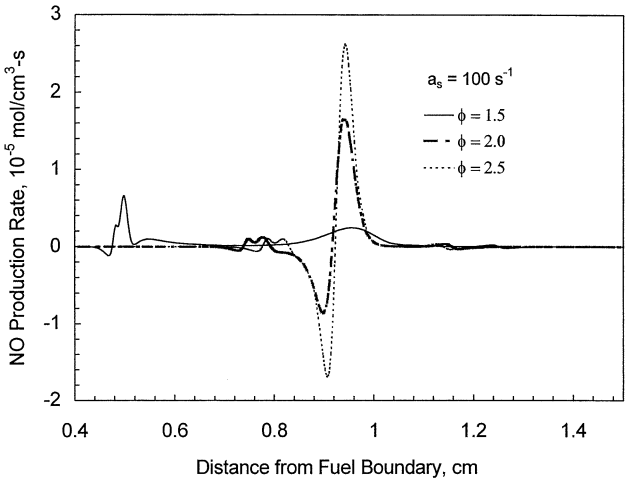

Fig. 6. NO production rate profiles for three PPFs discussed in the context of Fig. 5.

to the higher temperature and higher concentration of O and OH radicals in the non-premixed zone.

Figure 9 presents the integrated production rates of NO for the three mechanisms as functions of ϕ. As ϕ is increased, the NO production/consumption rates in the rich premixed zone decrease, while those in the non-premixed zone increase. This is consistent with the discussion presented earlier in the context of Figs. 5–7. More importantly, as ϕ is increased, the net NO production rate decreases slightly even though the NO production/consumption rates for all three mechanisms increase. This is due to the fact that the reburn NO production rate increases faster compared with those of thermal and prompt as ϕ is increased.

4.5. The NOx emission index

The effects of ϕ and a_s on NOx are summarized in Fig. 10, which presents the NOx emission index (EINOx), defined in Eq. 1, plotted versus ϕ for different strain rates. Two distinct regimes can be identified. In the first regime, represented by $\phi < 2.2$, EINOx exhibits strong sensitivity to variations in ϕ and a_s, while in the second regime ($\phi > 2.2$), where the two reaction zones are in the process of merging, EINOx is relatively less sensitive to both ϕ and a_s. Moreover, in the first regime, the effect of partial premixing on emission index is qualitatively different at low and high strain rates. For $a_s = 50\ s^{-1}$, which is representative of low-strain-rate flames, as ϕ is increased (i.e., the degree of partial premixing is decreased), EINOx first increases and then decreases, showing a maximum near $\phi = 2.2$. This behavior is qualitatively similar to that reported by Blevins and Gore [9] and Li and Williams [11] for methane-air PPFs at low strain rates. In contrast, for moderate- and high-strain-rate flames, the plot of EINOx versus ϕ exhibits a local minimum near $\phi = 1.8$.

To further examine the dependence of EINOx on ϕ and a_s, we plot in Fig. 11 the integrated NOx production and fuel consumption rates, normalized by their respective values at $\phi = 1.5$, as functions of ϕ for strain rates of 50 and 100 s^{-1}. As ϕ is increased, the fuel consumption rate first decreases ($\phi < 2.2$) and then increases slowly. The variation of fuel consumption rate is determined by the total fuel flow rate that increases with ϕ, and by the amount of unburned fuel escaping the flame that depends on the location of the premixed reaction zone with respect to the fuel nozzle. For $\phi < 2.2$, as ϕ is increased, the premixed reaction zone becomes weaker and moves farther away from the nozzle, and, consequently, the amount of fuel escaping the flame increases. This decreases the fuel consumption rate even though the fuel-flow rate increases with ϕ. For $\phi > 2.2$, however, the premixed reaction zone is in the process of merging with the non-premixed zone, and the fuel consumption rate increases,[4] albeit slowly, because the fuel flow rate increases with ϕ. The effect of increasing the strain rate is to increase the fuel consumption rate, primarily due to the higher fuel flow rate. It should be noted, however, that the ratio of fuel consumption rate to fuel flow rate (not shown) decreases as a_s is increased.

As indicated in Fig. 11, the NOx production rate as a function of ϕ exhibits opposite behavior for low- and high-strain-rate flames. For low-strain-rate flames ($a_s = 50\ s^{-1}$), as ϕ is increased, the NOx production rate increases to a maximum value and then decreases slowly, while for $a_s = 100\ s^{-1}$, it decreases to a minimum and then increases. To examine this behavior, we present in Fig. 12 the profiles

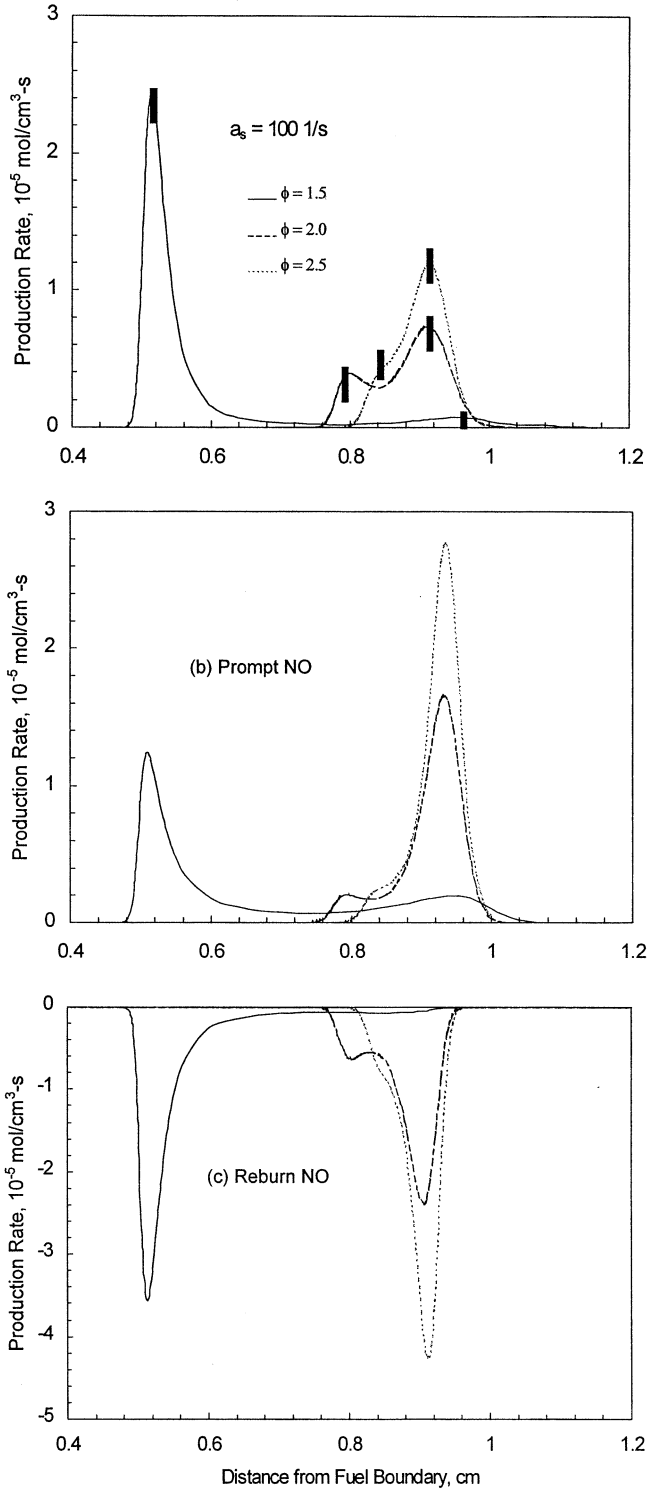

Fig. 7. Production rate profiles of (a) thermal, (b) prompt and (c) reburn mechanisms at $\phi = 1.5$, 2.0, 2.5, and $a_s = 100\ s^{-1}$. The vertical bars in Fig. 7a indicate the locations of the two-reaction zones.

Table 2
Relative contribution of thermal and prompt mechanisms at different ϕ, and a fixed $a_s = 100\ s^{-1}$

	$\phi = 1.5$	$\phi = 2.0$	$\phi = 3.0$
Contribution of Thermal NO (%)	50	40	35
Contribution of Prompt NO (%)	50	60	65

of temperature and of thermal and prompt NO formation rates for partially premixed flames established at $\phi = 1.5$ and 2.0, and a strain rate of 50 s^{-1}. The corresponding results for $a_s = 100\ s^{-1}$ are presented in Fig. 7. Because the net production rate of NO_2 is less than 2% of NOx, the following discussion focuses on NO to characterize the EINOx behavior.

4.6. NOx emission index for low-strain-rate flames

For $a_s = 50\ s^{-1}$ and $\phi = 1.5$, the propagation speed of the premixed reaction zone is sufficiently high due to the high level of partial premixing. Consequently, as indicated in Fig. 12, the premixed zone is located close to the fuel boundary, resulting in a non-negligible heat loss to the boundary. As ϕ is increased from 1.5 to 2.0, it decreases the propagation speed of the premixed zone, and makes this zone move away from the fuel boundary or closer to the non-premixed zone. This reduces the heat loss to the fuel boundary, which is indicated by an increase in the premixed zone temperature (T_p), corresponding to the location where the NO formation rate has the highest value, from 1780°K to 1820°K. This, however, has a negligible effect on the total NO formation rate. A more important effect of the movement of

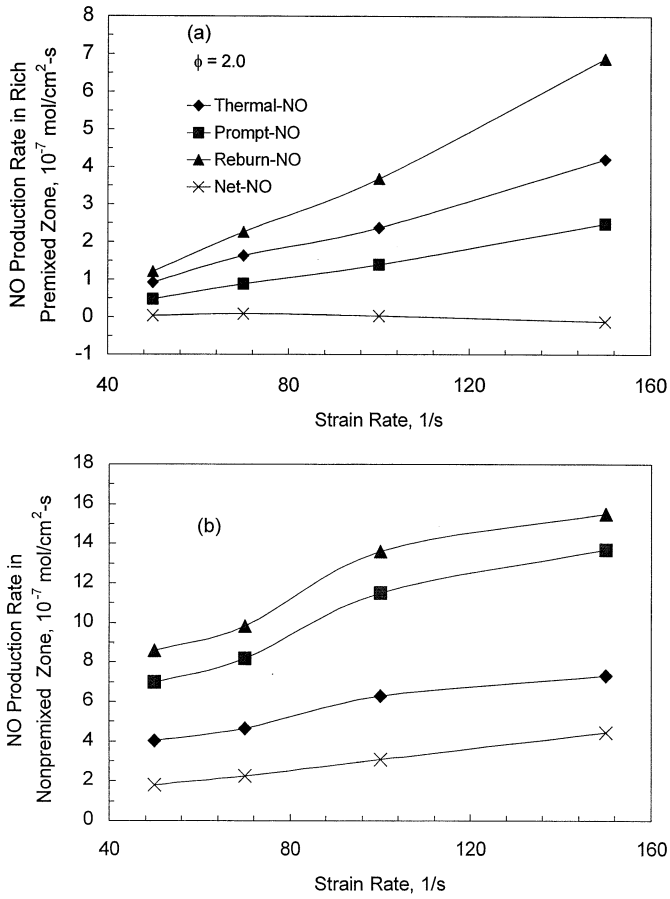

Fig. 8. The integrated production rates of thermal, prompt, reburn and the net NO plotted versus a_s in (a) the rich premixed and (b) non-premixed reaction zones.

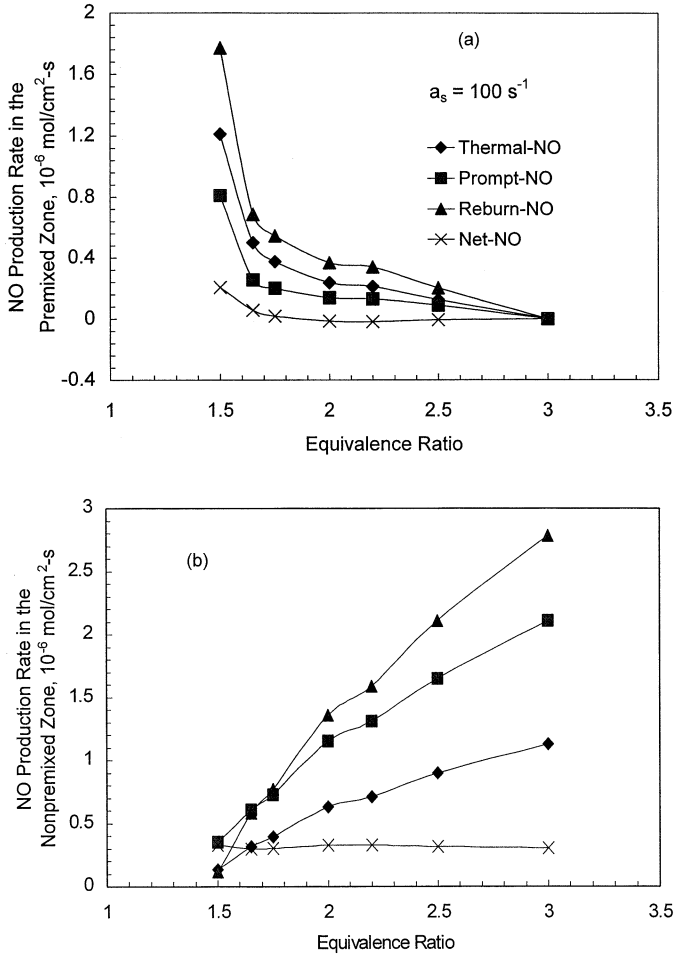

Fig. 9. The integrated production rates of thermal, prompt, reburn and the net-NO plotted versus ϕ in the (a) rich premixed and (b) non-premixed reaction zones.

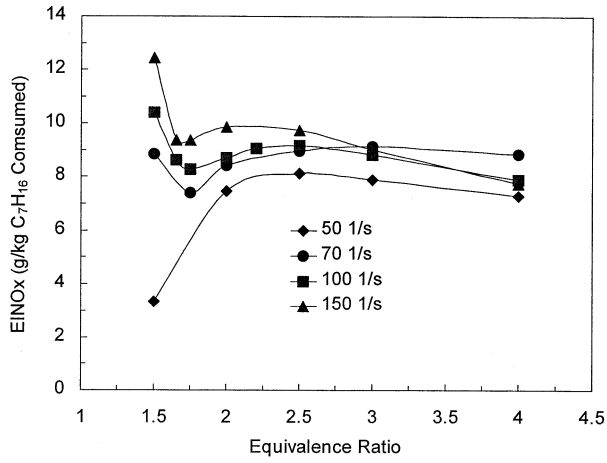

Fig. 10. NOx emission index plotted versus ϕ for different strain rates.

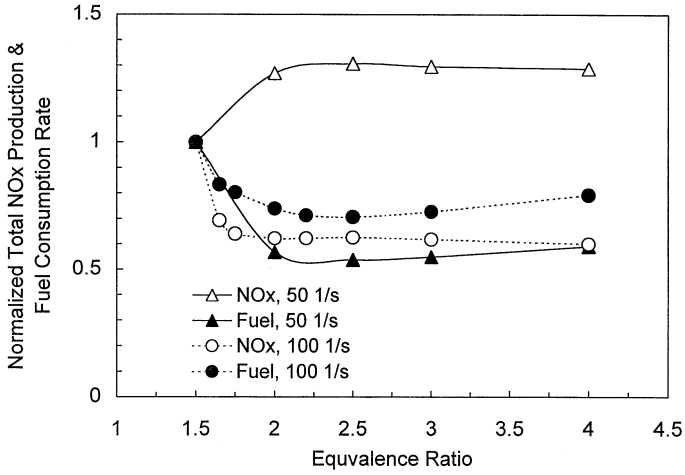

Fig. 11. Total normalized NOx production and fuel consumption rates plotted versus equivalence ratio for two strain rates.

the premixed zone is due to the enhanced interactions between the two reaction zones, caused by the reduced separation distance between them. These interactions are depicted more clearly in Fig. 13, which presents the profiles of temperature and H, OH, CO, and C_2H_2 species for $\phi = 1.5$ and 2.0. For $\phi = 1.5$, the premixed reaction zone is relatively strong and located far from the non-premixed zone. Consequently, the major interaction between the two zones corresponds to the transport of CO and H_2 form the premixed zone to the non-premixed zone. More importantly, there is no transport of C_2H_2 from the premixed zone to non-premixed zone, and, consequently, the prompt NO formation rate in the latter zone is negligibly small, see Fig. 12. The thermal NO formation rate in this zone is also small due to the reduced radical activity. Consequently, the total NO formation rate for this case is small, as indicated in Fig. 11. As ϕ is increased from 1.5 and 2.0, interactions between the two reaction zones are noticeably enhanced due to the reduced separation distance between them and the transport of C_2H_2 to the non-premixed zone becomes significant, see Fig. 13b. This causes a significant increase in the prompt NO formation rate in the non-premixed zone, as indicated in Fig. 12. The thermal NO formation rate in this zone is also enhanced due to higher radical activity. Consequently, as ϕ is increased, the total NO formation rate increases (cf. Figure 11), which leads to higher EINOx because the fuel consumption rate decreases. This trend does not continue, however, as ϕ is increased further, because the two reaction zones are close to merging. For $\phi > 2.2$, the total NO formation rate becomes nearly constant with ϕ, and because the fuel

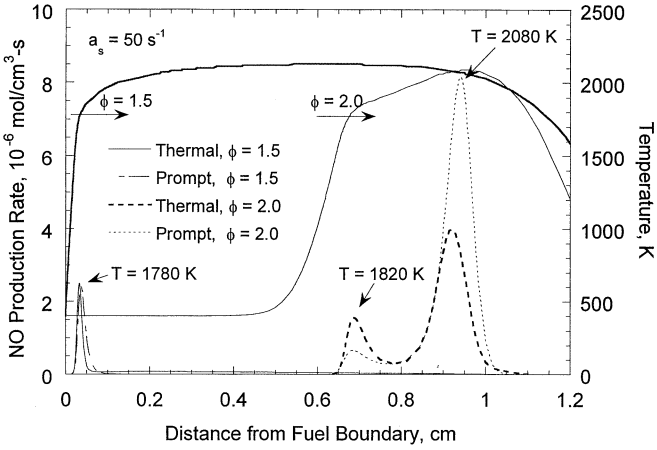

Fig. 12. Profiles of temperature and those of thermal and prompt NO formation rates for partially premixed flames established at $\phi = 1.5$ and 2.0, and strain rate of 50 s^{-1}.

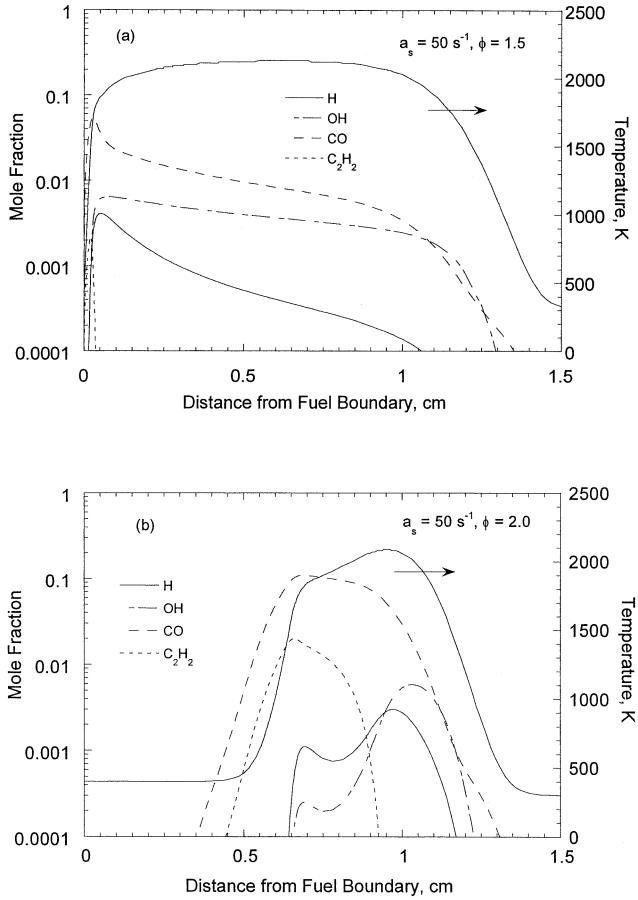

Fig. 13. Flame structures in terms of the profiles of temperature and species mole fractions for partially premixed flames at (a) $a_s = 50\ s^{-1}$, $\phi = 1.5$, and (b) $a_s = 50\ s^{-1}$, $\phi = 2.0$.

consumption rate now increases with ϕ, the NOx emission index decreases with ϕ, as indicated in Fig. 10.

It is also important to note that a similar behavior is observed when the strain rate is increased from a relatively low value ($a_s = 50\ s^{-1}$) for partially premixed flames established at relatively low equivalence ratios. Figure 14 presents the flame structures for $\phi = 1.5$ and $a_s = 50$ and $100\ s^{-1}$. As the strain rate is increased, the separation distance between the two reaction zones decreases, increasing the interaction between them. In particular, the transport of acetylene from the premixed zone to non-premixed zone becomes significant, and, consequently, the rate of NO formation in the non-premixed zone increases significantly, as indicated in Fig. 8b. As a result, EINOx increases as the strain rate is increased, see Fig. 10. This result, however, is in contradiction with that of Nishioka et al. [10] for methane-air partially premixed flames. The discrepancy is somewhat surprising because results of the two studies are in agreement concerning the effect of ϕ on EINOx for low-strain-rate flames. The discrepancy may be due to different parameters and boundary conditions used in the two studies. Another potential source of discrepancy is due to the chemistry models used. The Held and Dryer model employed in the present study has been shown to over-predict the C_2H_4 concentration [11, 32], which is the major source of C_2H_2. Because the transport of acetylene to the non-premixed zone is shown to represent an important process in determining the relative contributions of the thermal, prompt, and reburn mechanisms, it could modify the quantitative results. However, the qualitative results regarding the effects of a_s and ϕ on NOx emissions are expected to be the same using more comprehensive chemistry models [16, 33]

4.7. NOx emission index for moderate- and high-strain-rate flames

As indicated in Fig. 10, the NOx emission index exhibits a different behavior for moderate- and high-

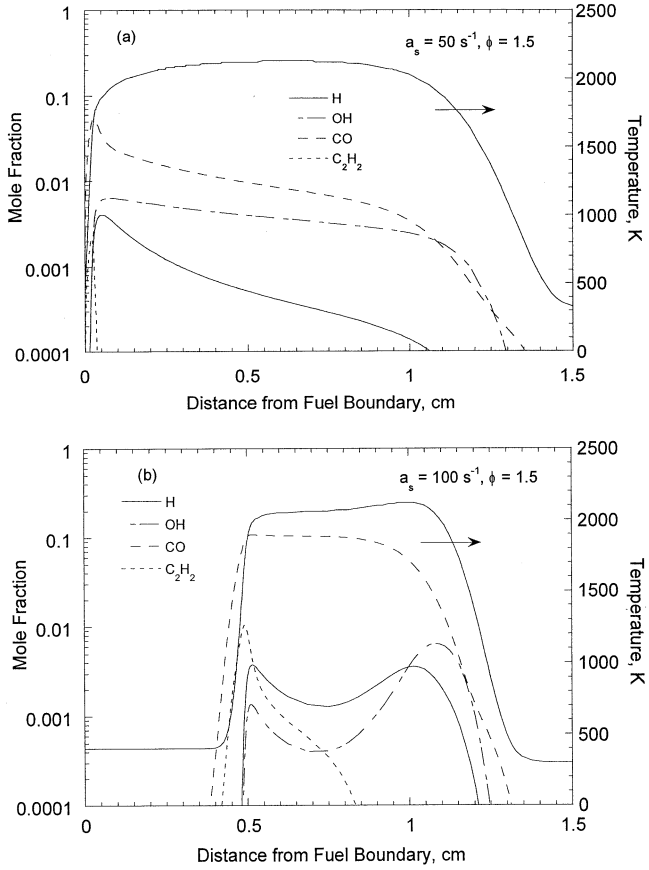

Fig. 14. Flame structures in terms of the profiles of temperature and species mole fractions for partially premixed flames at (a) $a_s = 50\ s^{-1}$, $\phi = 1.5$, and (b) $a_s = 100\ s^{-1}$, $\phi = 1.5$.

strain-rate flames compared to that for low-strain-rate flames ($a_s = 50\ s^{-1}$). For the latter case ($a_s \geq 70\ s^{-1}$), as ϕ is increased, EINOx first decreases to a local minimum value near $\phi = 1.8$, then increases to a local maximum value, and then decreases slowly as the equivalence ratio approaches the non-premixed flame limit. This result is in qualitative agreement with the measurements of Gore and Zhan [7] for methane-air, axisymmetric PPFs, and with the predictions of Berta et al. [15] using a more comprehensive n-heptane mechanism. This behavior can be explained by the results presented in Figs. 9 and 11. The effect of increasing ϕ is to weaken the premixed reaction zone, which decreases the NO formation rate in this zone, as indicated in Fig. 9a. Concurrently, the NO formation rate in the non-premixed reaction zone is also reduced due to the sharp increase in the NO consumption rate through the reburn mechanism, see Fig. 9b. Consequently, as ϕ is increased from 1.5 to 1.8, the total NO formation rate decreases sharply. As indicated in Fig. 11, for $a_s = 100\ s^{-1}$, both the fuel consumption rate and NOx production rate decrease with ϕ, but the latter decreases faster for $1.5 < \phi < 1.8$, and consequently, the NOx emission index decreases with ϕ. For $\phi > 1.8$, the reduction in fuel consumption rate becomes more dominant than that in NO production rate, and, consequently, EINOx increases with ϕ, as indicated in Fig. 10. After EINOx reaches a local maximum value near $\phi = 2.2$, it then decreases slowly as ϕ approaches the non-premixed flame. This can be attributed to the fact that the fuel consumption rate is now increasing with ϕ (cf. Fig. 11), while the NOx production rate is nearly independent of ϕ in the non-premixed limit.

Another important observation from Fig. 10 is that the equivalence ratio corresponding to the minimum EINOx point decreases with the strain rate for strain rates of 70, 100, and 150 s^{-1}. This is attributable to the fact that the critical equivalence ratio for the merging of the two reaction zones decreases with strain rate. The effect of strain rate on the critical equivalence ratio for merging has been discussed in our previous study [20].

5. Conclusions

The NO_x emission characteristics of heptane-air partially premixed flames have been investigated. The flame has been computed using a detailed mechanism combining the Held's n-heptane mechanism and the Li and Williams' NO_x mechanism. Both of these mechanisms have been validated in a reasonably comprehensive manner. The ROPA method has been employed to identify the dominant pathways and associated mechanisms for NOx formation and destruction in PPFs. The dominant mechanisms are found to be the thermal, prompt, and reburn mechanisms. Important reactions associated with these mechanisms are also identified.

A detailed investigation has been conducted to characterize NOx emissions under conditions for which the flame consists of two spatially separated reaction zones. For most conditions, the rate of NO formation in the non-premixed zone is significantly higher than that in the rich premixed zone. This can be attributed to two factors. The first is the transport of acetylene from the rich premixed to the non-premixed reaction zone, which provides CH radicals, and, thus enhances prompt NO formation in the latter zone. The second is the higher concentration of O and OH radicals in the non-premixed zone compared to that in the rich premixed zone, which enhances both the thermal and prompt NO formation in the non-premixed zone. For relatively high level of partial premixing ($\phi \leq 1.5$), however, the rate of NO formation in the rich premixed zone exceeds that in the non-premixed zone.

There is a significant NOx destruction region sandwiched between the rich and non-premixed reaction zones. The destruction occurs mainly through the reburn mechanism, and is caused by the transport of acetylene to the non-premixed zone; the acetylene form CH and CH_2 radicals that consume NO to form HCN and HNCO in the region upstream of this zone. From the consideration of reducing NOx in combustion systems that rely on partially premixed combustion, results suggest that the paucity of oxidizer in the region between the two reaction zones be promoted, as it enhances the NO destruction reactions in the region.

In the rich premixed zone, the contribution of thermal NO is generally higher than that of prompt NO, while in the non-premixed zone, the prompt NO is the major contributor. This behavior is again related to the transport of acetylene to the non-premixed zone, and higher concentrations of CH, O, and OH radicals in this zone. The relative contributions of thermal and prompt mechanisms to the total NOx is generally insensitive to variations in a_s, but has strong sensitivity to variations in ϕ.

The NOx emission index (EINOx) has been computed as a function of ϕ and a_s. Two distinct regimes are identified. In the first regime, represented by $\phi < 2.2$ and characterized by the presence of two spatially separated reaction zones, EINOx exhibits strong sensitivity to variations in ϕ or a_s. In the second regime, $\phi > 2.2$, EINOx is relatively insensitive to variations in ϕ and a_s. Here the two reaction zones are close to merging, and EINOx decreases slowly as ϕ approaches the non-premixed flame limit.

In the first regime, the plot of EINOx versus ϕ exhibits opposite behavior for low- and high-stain-rate flames. For low-stain-rate flames, EINOx increases and then decreases with ϕ, showing a maximum value near $\phi = 2.2$. This behavior is qualitatively similar to that reported by Blevins and Gore and Li and Williams for methane-air PPFs at low strain rates. In contrast, for moderate- and high-strain-rate flames, the plot of EINOx versus ϕ exhibits a local minimum near $\phi = 1.8$. This result is in qualitative agreement with the measurements of Gore and Zhan for methane-air, axisymmetric PPFs, and with the predictions of Berta et al. based on a more comprehensive n-heptane mechanism. Our simulations also indicate that the reburn NO mechanism plays an important role for these conditions. However, it is important to note that a significant amount of fuel bypasses the flame in a counter-flow configuration, and, therefore, conclusions regarding EINOx may be somewhat configuration-specific. Consequently, a direct comparison of our predictions with the measurement of EINOx reported by Gore and Zhan may not be meaningful due to different configurations used in the two studies.

Finally, two points are worth mentioning. First, our study clearly indicates that prompt NO requires the existence of not only CH but also O and OH radicals. There seems to be a prevailing notion in the literature that the existence of CH automatically implies that prompt NO will form. This notion should be corrected based on our results. Second, for moderate- and high-strain-rate partially premixed flames, there is an optimum value of equivalence ratio for which the NOx emission index is minimized. Although, the existence of an optimum ϕ has also been reported by previous investigations dealing with methane-air partially premixed flames, additional experimental and numerical studies are needed to further quantify this aspect. Future numerical studies should also focus on the effect of chemistry models on the relative contributions of the various NOx mechanisms, as well as on the NOx emission index. In particular, the sensitivity of the predicted C_2H_4 and C_2H_2 concentrations to the chemistry model should be quantified, because the transport of acetylene to the non-premixed zone is found to have a

major effect on the predicted NOx emissions in n-heptane partially premixed flames. More comprehensive models of Curran et al. and Lindstedt and Maurice should be used for this analysis. Also the effects of multidimensionality on NOx characteristics of heptane-air partially premixed flames should be discussed. Nishioka et al. [34] have examined this issue for methane-air co-flow partially premixed flames.

Notes

1. It is important to distinguish between the overall equivalence ratio and the fuel-rich mixture equivalence ratio for partially premixed flames. The equivalence ratio in the present study refers to the latter, and is denoted as ϕ.
2. CH radicals are also consumed in the hydrocarbon chemistry that leads to the formation of CO.
3. Note at very low strain rates, there is non-negligible heat loss to the burner due to the close proximity of the rich premixed reaction zone to the fuel nozzle.
4. Note for $\phi \geq 2.5$ the ratio of fuel consumption rate to fuel flow rate (not shown) still decreases with increasing ϕ.

Acknowledgments

This research was supported by the NSF Combustion and Plasma Systems Program for which Dr. Farley Fisher is the Program Director. Professor F. L. Dryer and Dr. T. Held provided the n-heptane mechanism, along with many insights during this research. Many fruitful discussions with Professor I. K. Puri are gratefully appreciated. Several useful comments from the reviewers, especially from reviewer 2, and Professor T. Bowman have enhanced the quality of this work.

References

[1] F.F. Flynn, R.P. Durrett, G.L. Hunter, et al., Diesel Combustion: An Integrated View Combining Laser Diagnostics, Chemical Kinetics, and Empirical Validation, SAE, Paper 99-01-0509, 1999.
[2] B.J. Lee, S.H. Chung, Combust. Flame 109 (1997) 163.
[3] L. Vervisch, Proceedings of the Combustion Institute, Vol. 28, The Combustion Institute, Pittsburgh, 2000, p. 11.
[4] Z. Shu, B.J. Krass, C.W. Choi, S. Aggarwal, V.R. Katta, I.K. Puri, Twenty-Seventh Symposium (International) on Combustion, The Combustion Institute, Pittsburgh, 1998, p. 625.
[5] R. Azzoni, S. Ratti, S.K. Aggarwal, I.K. Puri, Combust. Flame 119 (1999) 23.
[6] H. Xue, S.K. Aggarwal, AIAA J. 39 (4) (2001) 637.
[7] J.P. Gore, N.J. Zhan, Combust. Flame 105 (1996) 414–427.
[8] T.K. Kim, B.J. Alder, N.M. Laurendeau, J.P. Gore, Combust. Sci. Tech. 111 (1995) 361.
[9] L.G. Blevins, J.P. Gore, Combust. Flame 116 (1999) 546.
[10] M. Nishioka, S. NakaGawa, Y. Ishikawa, T. Takeno, Combust. Flame 98 (1994) 127.
[11] S.C. Li, F.A. Williams, Combust. Flame 118 (1999) 399.
[12] Q.V. Nguyen, R.W. Dibble, C.D. Carter, G.J. Fiechtner, R.S. Barlow, Combust. Flame 105 (1996) 499.
[13] R.V. Ravikarishna, N.M. Laurendeau, Combust. Flame 122 (2000) 474.
[14] S.C. Li, F.A. Williams, Proceedings of the Combustion Institute, Vol. 28, The Combustion Institute, Pittsburgh, 2000, p. 1031.
[15] P. Berta, A. Mukhopadhyay, I.K. Puri, S. Granata, T. Faravelli, E. Ranzi, Effect of Partial Premixing on NOx and Soot Formation in Heptane-Air Flames, Proceeding of the Technical Meeting of the Central State Section of the Combustion Institute, Knoxville, USA, 2002.
[16] R.P. Lindstedt, L.Q. Maurice, Detailed kinetic modeling of n-heptane combustion. Combust. Sci. Tech. 107 (1995) 317.
[17] T.J. Held, A.J., Marchese, F.L. Dryer, Comb. Sci. Tech. 123 (1997) 107.
[18] A.J. Marchese, F.L. Dryer, V. Nayagam, Combust. Flame 116 (1999) 432.
[19] A.E. Bakali, J. Delfau, C. Vovelle, Combust. Flame 118 (1999) 381.
[20] H. Xue, S.K. Aggarwal, AIAA J. 40 (11) (2002) 2289.
[21] A.E. Lutz, R.J. Kee, J.F. Grcar, F.M. Rupley, OPPDIF: A FORTRAN Program for Computing Opposed-Flow Diffusion Flames, Technical Report SAND96-8243, UC-1404, 1997.
[22] R.J. Kee, F.M. Rupley, J.A. Miller, Chemkin: A FORTRAN Chemical Kinetics Package for the Analysis of Gas Phase Chemical Kinetics, Technical Report SAND89-8009B, 1989.
[23] G.P. Smith, D.M. Golden, M. Frenklach, N.W. Moriarty, B. eiteneer, M. Goldenberg, C.T. Bowman, R.K. Hanson, S. Song, W.C. Gardiner, V.V. Lissianski, Z. Qin, GRI Mech-3.0, http://www.me.berkeley.edu/grimech/.
[24] J. Warnatz, P. Klaus, CEC Reaction Mechanism for the Methane/Air Combustion, http://www.ca.sandia.gov/tdf/3rdWorkshop/ChemMech/JW-C2NO98.mec.html.
[25] Leeds NO_x Mechanism, http://www.chem.leeds.ac.uk/Combustion/nox.html.
[26] J.A. Miller, C.T. Bowman, Prog. Energy Combust. Sci. 15 (1989) 287.
[27] P. Bajaj, Ph.D. Thesis, Eidgenössische Technische Hochschule Zürich, 2001.

[28] T. Takeno, M. Nishioka, Combust. Flame 92 (1993) 465–475.
[29] T. Turanyi, Kinalc Homepage, http://www.chem-.leeds.ac.uk/Combustion/kinalc.html.
[30] H. Xue, S.K. Aggarwal, NOx Emissions in n-Heptane/Air Partially Premixed Flames, 40th AIAA Aerospace Sciences Meeting and Exhibit, Reno, Nevada, 2002.
[31] M. Nishioka, Y. Kondoh, T. Takeno, Twenty-Sixth Symposium (International) on Combustion, The Combustion Institute, Pittsburgh, 1996, p. 2130.
[32] D.C. Horning, A Study of the High-Temperature Autoignition and Thermal Decomposition of Hydrocarbons, Ph.D. Thesis (Report No. TSD-135), Mechanical Engineering Department, Stanford University, 2001.
[33] H.J. Curran, P. Gaffuri, W. Pitz, C.K. Westbrook, Combust. Flame 114 (1998) 149.
[34] X. L. Zhu, M. Nishioka, T. Takeno, Twenty-Seventh Symposium (International) on Combustion, The Combustion Institute, Pittsburgh, 1998, p. 1369.